ACS Macro Letters

Letter

pubs.acs.org/macroletters

Injectable Interpenetrating Network Hydrogels via Kinetically Orthogonal Reactive Mixing of Functionalized Polymeric Precursors

Trevor Gilbert, Niels M. B. Smeets, and Todd Hoare*

Department of Chemical Engineering, McMaster University, 1280 Main Street West, Hamilton, Ontario L8S 4L7, Canada

Supporting Information

ABSTRACT: The enhanced mechanics, unique chemistries, and potential for domain formation in interpenetrating network (IPN) hydrogels have attracted significant interest in the context of biomedical applications. However, conventional IPNs are not directly injectable in a biological context, limiting their potential utility in such applications. Herein, we report a fully injectable and thermoresponsive interpenetrating polymer network formed by simultaneous reactive mixing of hydrazone cross-linked poly(*N*-isopropylacrylamide) (PNIPAM), and thiosuccinimide cross-linked poly(*N*-vinylpyrrolidone) (PVP). The resulting IPN gels rapidly (<1 min) after injection without the need for heat, UV irradiation, or small-molecule cross-linkers. The IPNs, cross-linked by kinetically orthogonal mechanisms, showed a significant synergistic enhancement in shear storage modulus compared to the individual component networks as well as distinctive pore morphology, degradation kinetics, and thermal swelling; in particular, significantly lower hysteresis was observed over the thermal phase transition relative to single-network PNIPAM hydrogels.

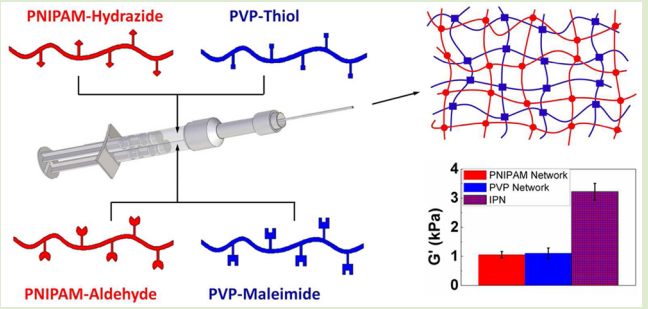

In biomedical applications of hydrogels such as tissue engineering and drug delivery, *in situ* gelation from injectable precursors is often desirable to avoid both the local trauma to the patient and the high costs associated with surgical implantation.[1] A variety of *in situ* reactive cross-linking chemistries active under physiological conditions have been reported for this purpose, including hydrazone bonding, the family of Michael-type additions, disulfide self-cross-linking of thiolated polymers, oxime formation, alkyne−azide "click" reactions, and Diels−Alder cycloadditions.[3] Hydrazone cross-links can be formed following reactive mixing of aldehyde-functionalized polymers and small-molecule dihydrazides[4] or hydrazide-functionalized polymers,[2b,c,5] with gelation occurring rapidly after mixing (seconds to minutes) and degradation occurring slowly (over months) at physiological pH.[2b,c,4a] In contrast, Michael addition between thiolated polymers and maleimides[2a,6] (to form thiosuccinimides), acrylates[7] (to form thioesters), or vinyl sulfones[8] (to form thioethers) is typically slower (ranging from minutes to tens of minutes)[9] and (when the N-substituent of the maleimide contains an amine) creates a linkage that is essentially nondegradable.[10] Of interest, the thiosuccinimide bond has been noted to form with high specificity and orthogonality to hydrazone bond formation at physiological pH,[11] with the thiosuccinimide and hydrazone linkages shown to be highly favored over any potential cross-reactive bonding.

Interpenetrating polymer networks (IPNs) are formed when the polymer volume fraction of two networks coexists within each other's free volume without the two networks being chemically bonded. The resulting interlocked network structure typically gives IPNs stiffer mechanical properties than corresponding single networks.[12] Network interpenetration also modulates the geometry and dimensions of the pore structure of the hydrogel, enabling regulation of diffusion into or through the gel phase.[5e,13] Furthermore, overlapping but chemically orthogonal networks can be designed such that the constituent networks degrade according to different kinetic profiles,[5e] allowing deliberate variation of properties over time[5e,13,14] potentially useful in tissue engineering applications. In the context of drug delivery, the composition, pore structure, and degradation properties of the two interpenetrating networks can be used to tune drug loading and release, including mitigation of the extent of the initial burst release which is typically problematic in hydrogel release vehicles.[13,15]

Traditional sequential or simultaneous methods of producing interpenetrating networks generally involve *in situ* polymerization from monomeric precursors.[16] However, gelation of functionalized prepolymers is generally more attractive in this context since it avoids the use of cytotoxic monomers and/or small-molecule initiators, heat, or UV treatment that may induce local or systemic toxicity.[2] While nominally injectable thermosensitive IPN systems have been reported that include monomeric precursors,[17] monomer toxicity is a particular concern in the polymerization of "smart" polymer precursors like *N*-isopropylacrylamide. UV-induced photogelation[18] may

Received: June 2, 2015
Accepted: September 10, 2015
Published: September 16, 2015

DOI: 10.1021/acsmacrolett.5b00362
ACS Macro Lett. 2015, 4, 1104−1109

also be logistically difficult in some *in vivo* environments and may induce local tissue damage at doses required for cross-linking.[18]

Recent work by Zhang et al., in which oxidized dextran and thiolated chitosan were orthogonally cross-linked via two independent chemistries, demonstrated the potential to modulate gel degradation based on the differing labilities of two independent bonds.[19] However, since one polymer pair was used to host both reactive cross-linking chemistries, the resulting product was a doubly cross-linked single network rather than a truly independent IPN gel. Similarly, semi-interpenetrating networks in which free polymer chains are entrapped in a cross-linked network (achievable via a variety of pathways of varying biological compatibility and ease of implantation[20]) lack the interlocked networks of a full IPN, which can significantly affect both the mechanical properties of the overall network and the environmental responses of IPNs based on pH- or thermosensitive polymers.[5e] Thus, a true injectable IPN that cross-links via orthogonal chemistries hosted on different precursor polymers would represent a new hydrogel architecture with potentially useful mechanical and environmentally responsive properties.

Herein, we describe the first fully injectable (i.e., both interpenetrating networks covalently gel upon mixing without any additional stimulus required), full interpenetrating network hydrogel comprised of a hydrazone cross-linked poly(*N*-isopropylacrylamide) (PNIPAM) network (previously demonstrated in our lab to form rapidly, degrade slowly, and elicit no significant cytotoxic, inflammatory, or capsule formation response through both in vitro and in vivo assays[4f]) interpenetrated with a thiosuccinimide cross-linked poly(*N*-vinylpyrrolidone) (PVP) network (Figure 1). The orthogonal gelation of the two constituent networks from a single double-barrel syringe administration results in an IPN with significantly enhanced mechanical properties and tunable thermal, degradation, and morphological properties according to the type of interpenetration achieved.

Small-molecule analogue NMR experiments confirmed that the hydrazide−aldehyde (Hzd-Ald) and thiol−maleimide (SH-Mal) dual cross-linking configuration meets the required kinetic orthogonality constraints for forming an IPN. Co-storage of the SH/Hzd analogues and the Mal/Ald analogues (Figures S1) for 40 days led to no significant peak changes over time, indicating the lack of reactivity between prepolymers coloaded into each barrel of the syringe. Furthermore, when equimolar amounts of the Hzd and Ald analogues were rapidly mixed with either the SH or Mal (Figures S2) analogues, the expected hydrazone bond forms to the exclusion of side products. Indeed, when the potential cross-reactive Hzd/Mal pair was tested in a binary mixture, trivial (<1%) reaction was observed over three days (Figure S4), suggesting that these gelling pairs are not just kinetically orthogonal but also largely chemically orthogonal. Thus, the intended hydrazone bond is highly favoured over any potential cross-reactions with thiol or maleimide, suggesting the potential utility of this pair of chemistries for the formation of an injectable interpenetrating network hydrogel. This is further supported by FT-IR data indicating the formation of similar bonds in both the single network controls and the IPN sample (Figures S5c, S5d), and solution-state NMR spectra of both IPN and single network control hydrogels, in which no additional peaks aside from those of the single network hydrogels were visible in the IPN spectrum (Figure S6).

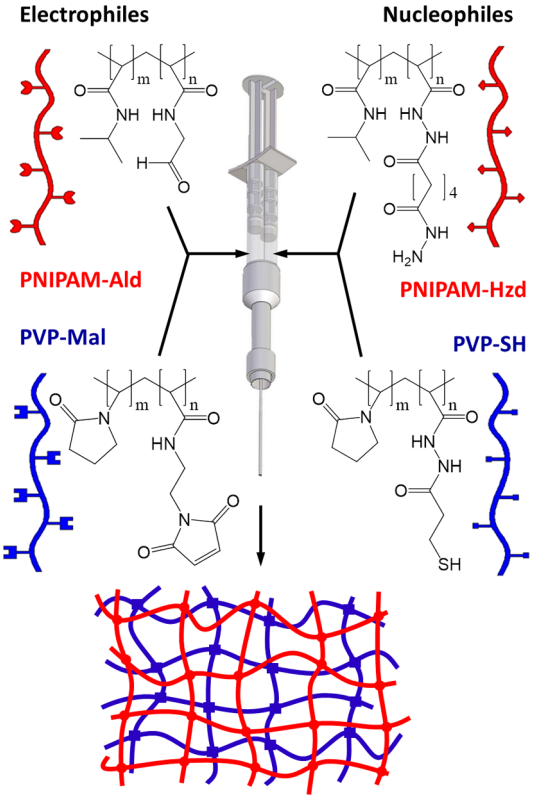

Figure 1. Schematic of chemistry and gelation strategy used for injectable IPN formation.

IPN hydrogels based on hydrazide and aldehyde-functionalized PNIPAM precursor polymers (PNIPAM-Hzd and PNIPAM-Ald, respectively) and thiol and maleimide-functionalized PVP precursor polymers (PVP-SH and PVP-Mal, respectively) were then formed by loading the electrophilic and nucleophilic components of each gelling mixture in separate barrels of a double-barrel syringe and coextruding the precursor reactive polymers through a static mixer into cylindrical silicone molds. Single network hydrogel controls, a full IPN of both networks, and a semi-IPN of free PVP (of comparable molecular weight as PVP-Mal and PVP-SH, Table S2) in a hydrazone cross-linked PNIPAM matrix were prepared (Table 1); the semi-IPN network enables clear distinguishing of

Table 1. Composition of Hydrogel Test Samples

hydrogel composition	barrel 1	barrel 2
PNIPAM	6 wt % PNIPAM-Hzd	6 wt % PNIPAM-Ald
PVP	9 wt % PVP-SH	9 wt % PVP-Mal
semi-IPN	6 wt % PNIPAM-Hzd	6 wt % PNIPAM-Ald
	9 wt % unfunctionalized PVP	9 wt % unfunctionalized PVP
IPN	6 wt % PNIPAM-Hzd	6 wt % PNIPAM-Ald
	9 wt % PVP-SH	9 wt % PVP-Mal

the synergistic effects of dual cross-linking in the full IPN relative to the effects of incorporating additional polymer mass in an interpenetrating phase. All compositions gelled in <1 min, with the higher concentration of the PVP-SH/PVP-Mal polymers used compensating for the slower inherent reaction kinetics of thiosuccinimide bond formation; as such, both interpenetrating networks are forming essentially simultane-

DOI: 10.1021/acsmacrolett.5b00362
ACS Macro Lett. 2015, 4, 1104−1109

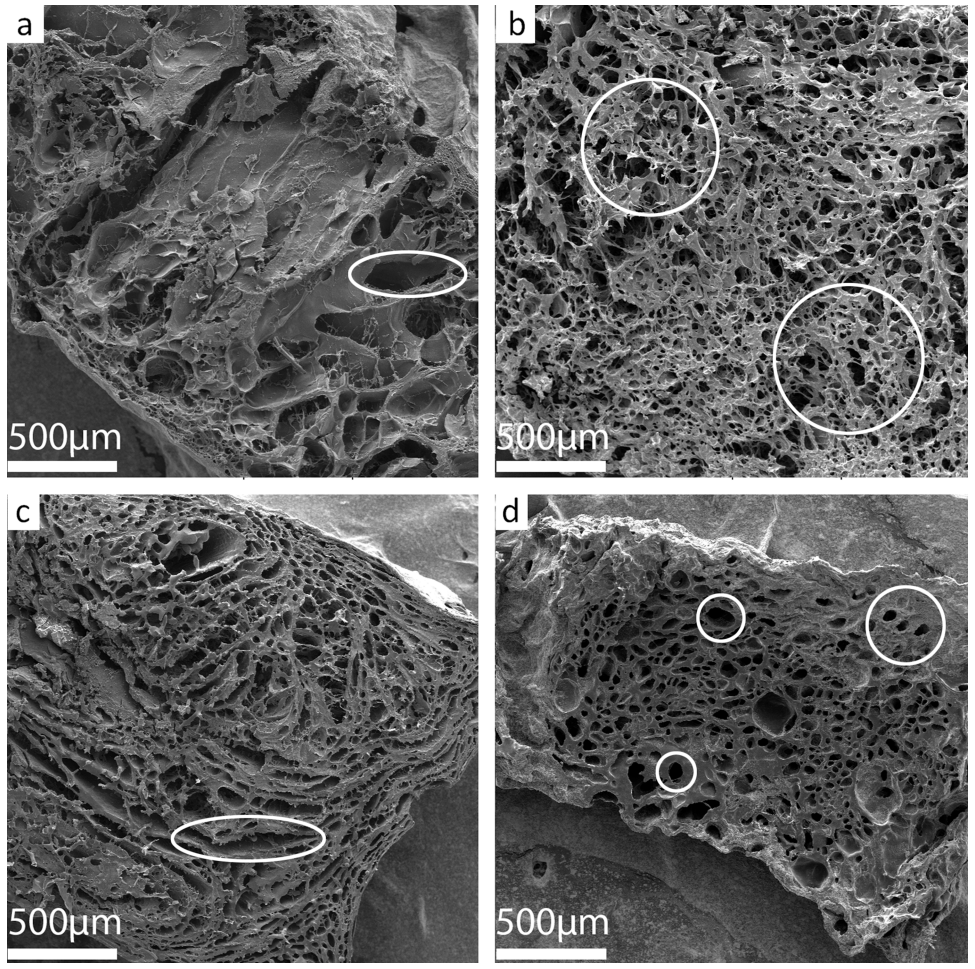

Figure 2. Scanning electron microscopy images of (a) PNIPAM single-network hydrogel, (b) PVP single-network hydrogel, (c) PNIPAM + unfunctionalized PVP semi-IPN hydrogel, (d) PNIPAM + PVP full IPN hydrogel.

ously but rapidly following coextrusion of the precursor polymers.

Morphological examination of the hydrogels by freeze-fracture SEM (Figure 2) shows considerable differences between the IPN and semi-IPN compared to the single-network controls. The IPN systems cleaved along a more sharply defined plane, consistent with their higher polymer concentration and stiffness. Both IPN and semi-IPN hydrogels show pore sizes closer to the smaller irregular pores in the PVP network (Figure 2b; circles) but with more defined boundaries similar to the larger pores in the PNIPAM control (Figure 2a; circles). In addition, the semi-IPN morphology is characterized by segments of flattened, lamellar pores more similar to the PNIPAM control (Figures 2a and 2c; ovals), while the full IPN sample tends toward more regularly rounded pore morphology consistent with the formation of a secondary network-forming component being present.

Comparison of the shear storage moduli of the individual hydrogel phases alone relative to the semi-IPN and full-IPN combinations of those hydrogels also indicates clear differences between the mechanics and thus morphologies of the different hydrogel networks (Figure 3). Note that a semi-IPN of unfunctionalized PNIPAM (again of similar molecular weight as PNIPAM-Hzd and PNIPAM-Ald, Table S2) in a thiosuccinimide cross-linked PVP was also prepared to confirm that gelation of both independent phases induced a significant mechanical synergism effect.

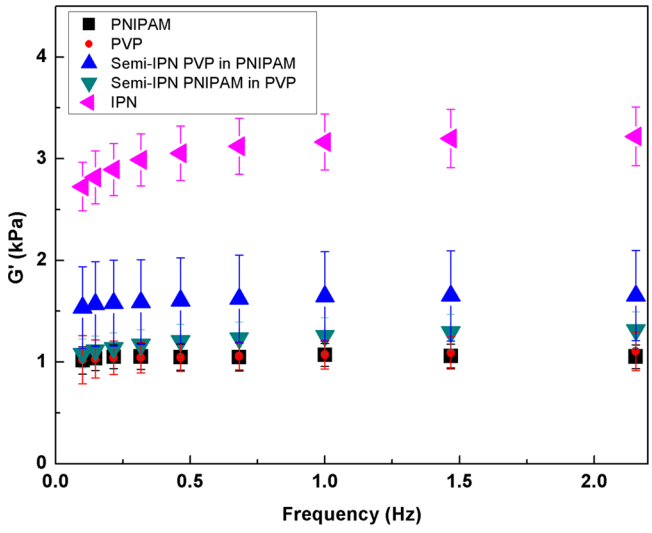

Figure 3. Shear storage modulus G' as a function of frequency for PNIPAM and PVP control hydrogels as well as the full IPN of those two networks and semi-IPN analogues prepared by entrapping linear PVP or PNIPAM into a hydrogel of the other polymer.

DOI: 10.1021/acsmacrolett.5b00362
ACS Macro Lett. 2015, 4, 1104−1109

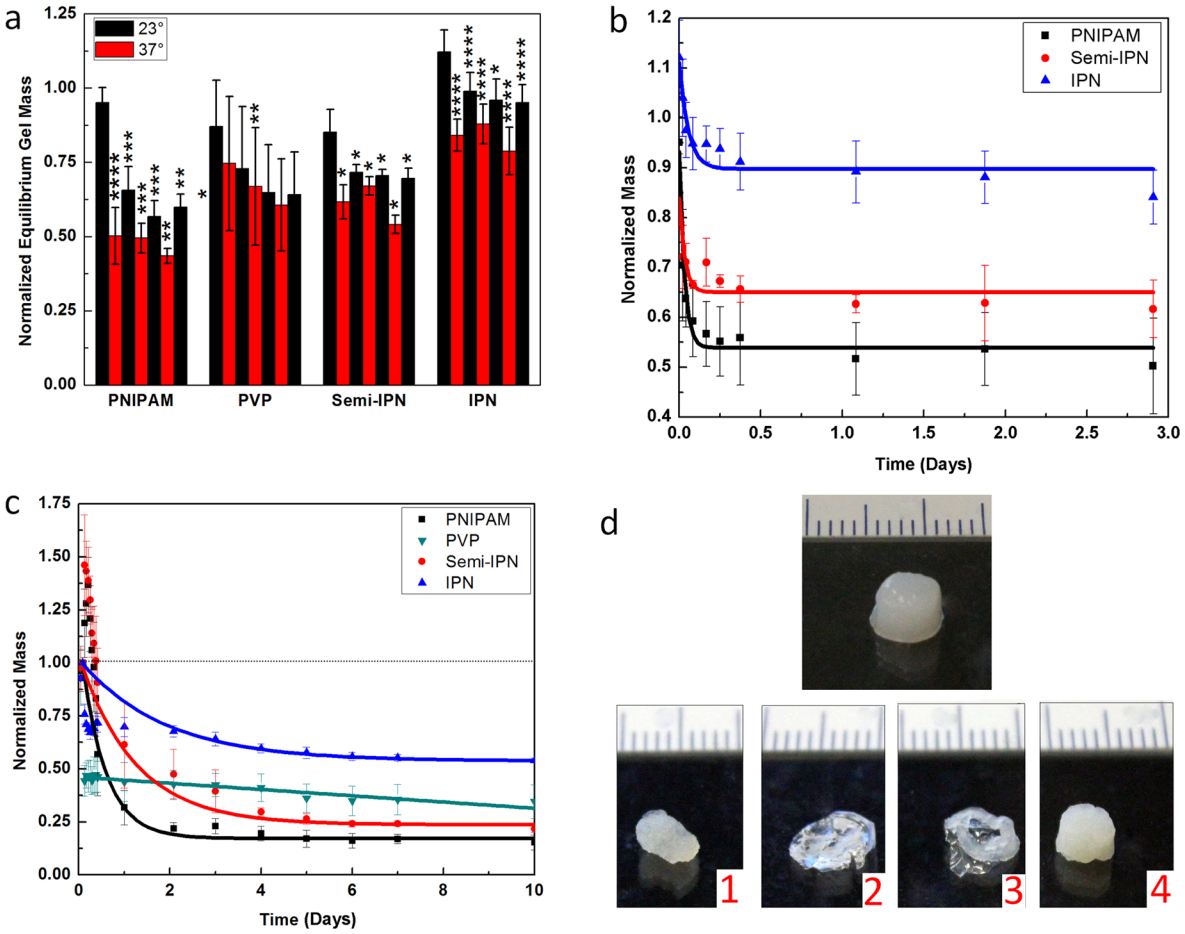

Figure 4. Swelling and degradation responses of injectable IPN hydrogels: (a) equilibrium swelling ratios (normalized to the hydrogel mass upon removal from mold) as a function of temperature for single-phase gels (PNIPAM, PVP) relative to semi-IPN and full-IPN gels over multiple heat−cool cycles (*$p < 0.05$; ** $p < 0.01$; *** $p < 0.005$; **** $p < 0.001$ for pairwise comparisons relative to the previous cycle); (b) deswelling kinetics for thermosensitive hydrogels pre-equilibrated at 23 °C transferred to a 37 °C shaking incubator (lines represent exponential best-fit trend lines, see Table S4; note that PVP single-network hydrogels showed no significant swelling changes over the course of the experiment and were thus omitted for clarity); (c) degradation of single-network, semi-IPN, and full IPN hydrogels in 0.1 M HCl (lines represent exponential best-fit trendlines, see Table S5); (d) Top: representative freshly molded hydrogel (PNIPAM). Bottom: (d-1) PVP, (d-2) PNIPAM, and (d-3) semi-IPN after 10 days in 0.1 M HCl and (d-4) IPN incubated in 0.1 M HCl for a full 42 days with minimal deformation.

Approximately equal storage modulus (G) values were observed for the PNIPAM and PVP single-network controls over the full frequency range tested. The semi-IPN containing free PVP showed a ∼60% enhancement in storage modulus compared to the PNIPAM-Hzd/PNIPAM-Ald control alone (ANOVA: $p < 10^{-65}$, $p < 0.05$ at each frequency measured), while the inverse IPN (free PNIPAM in a PVP matrix) displayed minimal enhancement in modulus relative to the single network hydrogels. In comparison, the full IPN hydrogel samples prepared with PVP-Mal/PVP-SH showed a ∼3-fold increase in storage modulus versus the PNIPAM or PVP control samples, with a modulus significantly (∼2-fold) higher than that of the semi-IPN control (ANOVA: $p < 10^{-48}$; t test: $p < 0.05$ for each frequency measured). Thus, the full IPN hydrogel shows a 50% higher G' value than that predicted by simply adding the constituent G' values of the control PNIPAM and PVP networks. Thus, the formation of an independently cross-linked interpenetrating PVP network provides synergistic reinforcement of the bulk hydrogel relative to that achieved by incorporating unfunctionalized PVP-based polymers, in which all potential intermolecular interactions aside from covalent cross-linking are still operable.

Cyclic swelling data between room temperature and 37 °C (expressed relative to the initial gel mass, Figure 4a, and the equilibrium swelling degree following the previous thermal cycle, Table S3) showed that both the semi-IPN and the IPN preserved the thermosensitive behavior of the PNIPAM control. However, the full IPN maintained a significantly higher degree of swelling over multiple thermal cycles than either the single-component control gels or the semi-IPN. Furthermore, the hysteresis observed over the first thermal cycle in the single-network PNIPAM hydrogel was significantly reduced in the semi-IPN and largely eliminated in the full IPN. We hypothesize these observations are both attributable to the interpenetrated cross-linked hydrophilic PVP network that elastically resists thermal deswelling of the PNIPAM network while also maintaining a higher overall degree of hydration inside the hydrogel; the latter effect is particularly important for reducing the potential for hydrogen bond formation between adjacent NIPAM residues upon chain collapse and thus promoting more reversible swelling−deswelling transitions.[21] Figure 4b (graph) and Table S4 (best-fit kinetics parameters) further indicate that the kinetic response of the IPN upon incubation at 37 °C is significantly slower than in the PNIPAM

DOI: 10.1021/acsmacrolett.5b00362
ACS Macro Lett. 2015, 4, 1104−1109

control, with the full-IPN also significantly slower than the semi-IPN consistent with the presence of a more hydrophilic, cross-linked interpenetrating phase. Overall, the interpenetrating hydrophilic PVP phase dampens the PNIPAM phase transition, suppresses bulk gel deswelling, and reduces hysteresis following the first heating cycle, with all effects enhanced in the fully cross-linked IPN relative to the semi-IPN consistent with the presence of a networked interpenetrating phase.

The hydrolytic degradation of the networks was assessed by immersion of gels in 0.1 M HCl to investigate the role of the semi-IPN and full IPN network structures on controlling network degradability (see Figure 4c for graph and Table S5 for best-fit kinetic parameters). The hydrazone cross-linked PNIPAM network is hydrolytically labile (particularly in acidic conditions), while the thiosuccinimide cross-linked PVP network is hydrolytically stable; such differential degradation potential may be useful in ultimate applications of these hydrogels in terms of dynamically tuning the mechanics or pore size of the gels as a function of time. Single-phase PVP hydrogels rapidly deswelled in 0.1 M HCl (likely due to rapid hydrolysis of residual maleimides to maleamic acid that can hydrogen bond with other gel residues)[22] but then remained stable over time, consistent with the irreversible nature of the ring-opened thiosuccinimide cross-link (Figure 4d-1). In contrast, an initial mass increase was observed in the first ∼6−12 h following acid incubation for the single-phase PNIPAM, semi-IPN, and full IPN networks due to swelling as the hydrazone cross-links begin to hydrolyze. Subsequently, the PNIPAM single network quickly degraded, with the hydrogel decomposing to fragments at the bottom of the weighing insert within 7 days of acid incubation (Figure 4d-2). The semi-IPN gels degraded slower and retained their shape to day 10 (Figure 4d-3), attributable to the modest mechanical reinforcement effect of the entrapped PVP (Figure 3) and/or the role of the interpenetrating PVP phase in immobilizing free water around the hydrazone cross-links. The IPN, in contrast, degrades much slower than the controls, retaining cylindrical sample geometry and 60% of its initial mass over 42 days of monitoring (Figure 4d-4). We anticipate that the thiosuccinimide cross-links of the PVP network preserve the macroscopic sample shape (analogous to the PVP control), with any degradation products from the hydrazone PNIPAM network captured inside the PVP network to form a semi-IPN of PNIPAM linear polymers in a PVP network over time. This demonstrated that modulation of the stability of the hydrazone cross-linked network using an interpenetrating network strategy is potentially useful for tuning the degradation time of a thermoresponsive hydrogel for targeted applications.

In summary, a novel method for creating a fully injectable, *in situ* gelling interpenetrating polymer network by orthogonal reactive mixing of functionalized polymer precursors has been demonstrated. Synergistic effects of the independently cross-linked networks were apparent in the mechanical properties, morphology, thermoresponsive swelling behavior, and degradation kinetics of the resulting IPN hydrogels. Given the capacity of IPNs to facilitate decoupled control over drug loading/release and degradation/mechanical properties of the network as a function of time, we anticipate such a chemistry and morphology may have particular utility for the prolonged release of small molecule hydrophilic or protein drugs with minimal convective burst and wound healing materials with both tissue adhesive and wound closing properties.

EXPERIMENTAL SECTION

Synthesis of Polymer Precursors. Hydrazide-functionalized PNIPAM (PNIPAM-Hzd) was prepared by conjugating adipic dihydrazide to PNIPAM-*co*-acrylic acid precursor polymers. Aldehyde-functionalized PNIPAM (PNIPAM-Ald) was synthesized by copolymerizing NIPAM with *N*-(2,2-dimethoxyethyl)methacrylamide and subsequently hydrolyzing the acetal moieties to aldehydes. Thiol- and maleimide-functionalized PVP (PVP-SH and PVP-Mal) were obtained from a common PVP-*co*-acrylic acid copolymer. PVP-SH was synthesized by conjugating 3,3′-dithiobis(propanoic dihydrazide) and cleaving the central disulfide bond with dithiothreitol. PVP-Mal was produced by conjugating *N*-(2-aminoethyl) maleimide via carbodiimide chemistry. See the Supporting Information for relevant NMR (Figures S1 and S2), FTIR (Figures S3 and S4), and degree of functionalization/molecular weight (Table S2) characterization of these precursor polymers.

IPN Preparation. Precursor polymers were loaded into a double-barrel syringe (sorted by electrophilic/nucleophilic properties). Hydrogels were formed via coextrusion of these precursor polymers into cylindrical silicone molds, covered on the top and bottom with glass microscope slides. Samples were stored overnight at room temperature in a sealed vessel saturated at 100% relative humidity to ensure equilibrium cross-linking prior to testing. Rheology samples were prepared using silicone molds of 12.7 mm diameter and 1.6 mm thickness; samples for all other tests were prepared using silicone molds of 3 mm diameter and 4.8 mm thickness.

Rheological Testing. Measurement of the storage modulus G' was carried out using the Mach-1 micromechanical testing system (Biomomentum). All samples (n = 4 per composition) were subjected to 20% precompression in the vertical axis. Stress sweeps were carried out to determine the linear viscoelastic regime of rotational amplitudes for each sample, followed by frequency sweeps within the linear viscoelastic region to determine G' and G''.

Freeze-Fracture Scanning Electron Microscopy (SEM). Hydrogel samples were rapidly frozen in liquid nitrogen and cut with a razor blade under a dissection microscope. Fractured hydrogel samples were then lyophilized, mounted on SEM sample holders using double-sided carbon tape and colloidal silver conductive paint, and sputter-coated with gold. SEM images were collected using a Vega LSU instrument (Tescan).

Swelling and Degradation Measurements. The thermoresponsive behavior of each of the four samples prepared (n = 4 per composition) was evaluated by tracking the overall mass change of the hydrogel (polymer + water) over multiple temperature cycles between 22 and 37 °C in 10 mM PBS at pH 7.4. Masses were normalized against the (hydrated) gel weights immediately after preparation (prior to incubation). As an accelerated simulation of degradation (for the purpose of comparison), mass changes were similarly tracked following incubation of the hydrogels in 0.1 M HCl at 22 °C. Samples were allowed to swell for 2 h in PBS, weighed as the basis for subsequent normalization, transferred to 0.1 M HCl, and weighed at predefined time points to track the kinetics of mass change in each hydrogel.

ASSOCIATED CONTENT

Supporting Information

The Supporting Information is available free of charge on the ACS Publications website at DOI: 10.1021/acsmacrolett.5b00362.

Full experimental methods, NMR spectra confirming orthogonality of gelling pairs, full polymer precursor characterization, and exponential best-fit parameters for the swelling kinetics and degradation kinetics experiments are provided (PDF)

DOI: 10.1021/acsmacrolett.5b00362
ACS Macro Lett. 2015, 4, 1104−1109

AUTHOR INFORMATION

Corresponding Author

*Phone: 1-905-525-9140 ext. 24701. E-mail: hoaretr@mcmaster.ca.

Notes

The authors declare no competing financial interest.

ACKNOWLEDGMENTS

The Natural Sciences and Engineering Research Council (NSERC), the Ontario Ministry of Research, and Innovation Early Researcher Award program (to TH) and the NSERC CREATE-IDEM (Integrated Design of Extracellular Matrices) program are gratefully acknowledged for funding. Nick Burke, Marcia West, and Katya D'Costa are thanked for their help with instrument training, consultation, and sample preparation.

REFERENCES

(1) Van Tomme, S. R.; Storm, G.; Hennink, W. E. *Int. J. Pharm.* **2008**, *355* (1−2), 1−18.

(2) (a) Fu, Y.; Kao, W. Y. J. *J. Biomed. Mater. Res., Part A* **2011**, *98A* (2), 201−211. (b) Patenaude, M.; Hoare, T. *ACS Macro Lett.* **2012**, *1* (3), 409−413. (c) Patenaude, M.; Hoare, T. *Biomacromolecules* **2012**, *13* (2), 369−378.

(3) Patenaude, M.; Smeets, N. M. B.; Hoare, T. *Macromol. Rapid Commun.* **2014**, *35* (6), 598−617.

(4) (a) Campbell, S. B.; Patenaude, M.; Hoare, T. *Biomacromolecules* **2013**, *14* (3), 644−653. (b) Dahlmann, J.; Krause, A.; Moller, L.; Kensah, G.; Mowes, M.; Diekmann, A.; Martin, U.; Kirschning, A.; Gruh, I.; Drager, G. *Biomaterials* **2013**, *34* (4), 940−951. (c) Hoare, T. R.; Kohane, D. S. *Polymer* **2008**, *49* (8), 1993−2007. (d) Martinez-Sanz, E.; Ossipov, D. A.; Hilborn, J.; Larsson, S.; Jonsson, K .B.; Varghese, O. P. *J. Controlled Release* **2011**, *152* (2), 232−240. (e) Patenaude, M.; Campbell, S.; Kinio, D.; Hoare, T. *Biomacromolecules* **2014**, *15* (3), 781−790. (f) Patenaude, M.; Hoare, T. *ACS Macro Lett.* **2012**, *1* (3), 409−413. (g) Patenaude, M.; Hoare, T. *Biomacromolecules* **2012**, *13* (2), 369−378. (h) Smeets, N. M. B.; Bakaic, E.; Patenaude, M.; Hoare , T. *Acta Biomater.* **2014**, *10* (10), 4143−4155. (I) Smeets, N. M. B.; Bakaic, E.; Patenaude, M.; Hoare , T. *Chem. Commun.* **2014**, *50* (25), 3306−3309. (j) Varghese, O. P.; Sun, W. L.; Hilborn, J.; Ossipov, D. A. *J. Am. Chem. Soc.* **2009**, *131* (25), 8781−8783.

(5) (a) Dahlmann, J.; Krause, A.; Moller, L.; Kensah, G.; Mowes, M.; Diekmann, A.; Martin, U.; Kirschning, A.; Gruh, I.; Drager, G. *Biomaterials* **2013**, *34* (4), 940−951. (b) Martinez-Sanz, E.; Ossipov, D. A.; Hilborn, J.; Larsson, S.; Jonsson, K. B.; Varghese, O. P. *J. Controlled Release* **2011**, *152* (2), 232−240. (c) Varghese, O. P.; Sun, W. L.; Hilborn, J.; Ossipov, D. A. *J. Am. Chem. Soc.* **2009**, *131* (25), 8781−8783. (d) Campbell, S. B.; Patenaude, M.; Hoare, T. *Biomacromolecules* **2013**, *14* (3), 644−653. (e) Hoare, T. R.; Kohane, D. S. *Polymer* **2008**, *49* (8), 1993−2007. (f) Patenaude, M.; Campbell, S.; Kinio, D.; Hoare, T. *Biomacromolecules* **2014**, *15* (3), 781−790. (g) Smeets, N. M. B.; Bakaic, E.; Patenaude, M.; Hoare, T. *Acta Biomater.* **2014**, *10* (10), 4143−4155. (h) Smeets, N. M. B.; Bakaic, E.; Patenaude, M.; Hoare, T. *Chem. Commun.* **2014**, *50* (25), 3306−3309.

(6) Nie, T.; Baldwin, A.; Yamaguchi, N.; Kiick, K. L. *J. Controlled Release* **2007**, *122* (3), 287−296.

(7) (a) Hiemstra, C.; van der Aa, L. J.; Zhong, Z. Y.; Dijkstra, P. J.; Feijen, J. *Biomacromolecules* **2007**, *8* (5), 1548−1556. (b) Metters, A.; Hubbell, J. *Biomacromolecules* **2005**, *6* (1), 290−301. (c) Salinas, C. N.; Anseth, K. S. *Macromolecules* **2008**, *41* (16), 6019−6026.

(8) (a) Lutolf, M. P.; Hubbell, J. A. *Biomacromolecules* **2003**, *4* (3), 713−722. (b) Qiu, B.; Stefanos, S.; Ma, J. L.; Lalloo, A.; Perry, B. A.; Leibowitz, M. J.; Sinko, P. J.; Stein, S. *Biomaterials* **2003**, *24* (1), 11−18. (c) Hiemstra, C.; van der Aa, L. J.; Zhong, Z. Y.; Dijkstra, P. J.; Feijen, J. *Macromolecules* **2007**, *40* (4), 1165−1173.

(9) Yu, Y. X.; Deng, C.; Meng, F. H.; Shi, Q.; Feijen, J.; Zhong, Z. Y. *J. Biomed. Mater. Res., Part A* **2011**, *99a* (2), 316−326.

(10) Lyon, R. P.; Setter, J. R.; Bovee, T. D.; Doronina, S. O.; Hunter, J. H.; Anderson, M. E.; Balasubramanian, C. L.; Duniho, S. M.; Leiske, C. I.; Li, F.; Senter, P. D. *Nat. Biotechnol.* **2014**, *32* (10), 1059−1062.

(11) Christie, R. J.; Anderson, D. J.; Grainger, D. W. *Bioconjugate Chem.* **2010**, *21* (10), 1779−1787.

(12) Naficy, S.; Kawakami, S.; Sadegholvaad, S.; Wakisaka, M.; Spinks, G. M. *J. Appl. Polym. Sci.* **2013**, *130* (4), 2504−2513.

(13) Zhang, X. Z.; Wu, D. Q.; Chu, C. C. *Biomaterials* **2004**, *25* (17), 3793−3805.

(14) (a) Lopes, C. M. A.; Felisberti, M. I. *Biomaterials* **2003**, *24* (7), 1279−1284. (b) Mandal, B. B.; Kapoor, S.; Kundu, S. C. *Biomaterials* **2009**, *30* (14), 2826−2836.

(15) Liu, Y. Y.; Fan, X. D.; Wei, B. R.; Si, Q. F.; Chen, W. X.; Sun, L. *Int. J. Pharm.* **2006**, *308* (1−2), 205−209.

(16) (a) Kong, X.; Narine, S. S. *Biomacromolecules* **2008**, *9* (5), 1424−1433. (b) Sperling, L. H. *Adv. Chem. Ser.* **1994**, *239*, 3−38.

(17) Zhao, J.; Zhao, X.; Guo, B. L.; Ma, P. X. *Biomacromolecules* **2014**, *15* (9), 3246−3252.

(18) Xiao, W. Q.; He, J. K.; Nichol, J. W.; Wang, L. Y.; Hutson, C. B.; Wang, B.; Du, Y. A.; Fan, H. S.; Khademhosseini, A. *Acta Biomater.* **2011**, *7* (6), 2384−2393.

(19) Zhang, H. W.; Qadeer, A.; Chen, W. *Biomacromolecules* **2011**, *12* (5), 1428−1437.

(20) (a) Berger, J.; Reist, M.; Mayer, J. M.; Felt, O.; Peppas, N. A.; Gurny, R. *Eur. J. Pharm. Biopharm.* **2004**, *57* (1), 19−34. (b) Kim, S.; Chung, E. H.; Gilbert, M.; Healy, K. E. *J. Biomed. Mater. Res., Part A* **2005**, *75A* (1), 73−88. (c) Zhou, Y. S.; Yang, D. Z.; Gao, X. Y.; Chen, X. M.; Xu, Q.; Lu, F. M.; Nie, J. *Carbohydr. Polym.* **2009**, *75* (2), 293−298.

(21) Ganji, F.; Vasheghani-Farahani, S.; Vasheghani-Farahani, E. *Iran Polym. J.* **2010**, *19* (5), 375−398.

(22) Matsui, S.; Aida, H. *J. Chem. Soc., Perkin Trans. 2* **1978**, No. 12, 1277−1280.

DOI: 10.1021/acsmacrolett.5b00362
ACS Macro Lett. 2015, 4, 1104−1109